# Synthesis and Characterization of New Anthracene-Based Semiconducting Polyethers

**K. Hriz,[1] N. Jaballah,[1] M. Chemli,[1] J. L. Fave,[2] M. Majdoub[1]**

[1]*Laboratoire des Polymères, Biopolymères et Matériaux Organiques, Faculté des Sciences de Monastir, Boulevard de l'Environnement, Monastir, Tunisia 5019*
[2]*Centre National de la Recherche Scientifique Unité Mixte de Recherche 7588, Institut des Nanosciences de Paris, Université Pierre et Marie Curie (Paris 06), 140 Rue de Lourmel, Paris, France 75015*

Received 28 December 2009; accepted 14 April 2010
DOI 10.1002/app.32659
Published online 18 August 2010 in Wiley Online Library (wileyonlinelibrary.com).

**ABSTRACT:** New anthracene-based polyethers, anthracene/bisphenol A (An–BPA) and anthracene/fluorinated bisphenol A (An–BPAF), were synthesized and characterized. An–BPA and An–BPAF were fully soluble in common organic solvents and had number-average molecular weights of 2580 and 3240, respectively. The optical properties of the polymers were investigated with ultraviolet–visible absorption and photoluminescence spectroscopy. Blue photoluminescence was observed in dilute solutions. In solid thin films, π–π interactions influenced the optical properties, and redshifted photoluminescence spectra were obtained; a green emission (504 nm) for An–BPAF and a green-yellow emission (563 nm) for An–BPA were found. By cyclic voltammetry, the electrochemical band gap was estimated to be 2.72 and 3.05 eV for An–BPA and An–BPAF, respectively. Single-layer diode devices of an indium tin oxide/polyether/aluminum configuration were fabricated and showed relatively low turn-on voltages (3.5 V for An–BPA and 3.7 V for An–BPAF). © 2010 Wiley Periodicals, Inc. J Appl Polym Sci 119: 1443–1449, 2011

**Key words:** conducting polymers; luminescence; polyethers; thin films

## INTRODUCTION

Enormous progress has been made in the investigation of organic, π-conjugated semiconducting materials in recent years.[1–3] These materials are classified into two types depending on the molecular size: conjugated polymers and so-called small conjugated molecules. Such functional compounds present promising organic analogues of silicon, the most exploited inorganic semiconductor. The main advantages of using organic semiconductors are their easy processability and low cost. These materials are in fact compatible with solution-processing techniques, and this eliminates the need for the expensive lithography and vacuum-deposition steps required for the elaboration of inorganic semiconducting films. Solution processing also expands the repertoire of tolerant substrates and processing options and allows flexible plastics to be used in conjunction with relatively simple methods such as spin coating (in the case of polymeric materials), stamping, and inkjet printing. The major characteristics of organic semiconducting materials are their tunable optoelectronic properties, which benefit from the richness of the organic synthesis and therefore from an adjustable molecular structure.[4,5] Currently, applications for organic semiconducting materials include thin-film transistors,[6,7] photovoltaic cells,[8] sensors,[9,10] organic lasers,[11] and especially organic light-emitting diodes (OLEDs).[12–14]

Anthracene was one of the first aromatic materials employed in OLED elaboration. The first experiments were carried out by Pope et al.[15] in the early 1960s. Soon after, several reports on single-crystal, anthracene-based OLEDs were published,[16,17] and good quantum yields were obtained (up to 5%). Nevertheless, such devices are thick and hence require very high operating voltages (>100 V). An improvement in the operating voltage was achieved by vacuum evaporation of thin layers of anthracene; in this case, the operating voltage was lowered up to 30 V.[18] However, anthracene tended to recrystallize with the diode operating time, and this led to a degradation of device performance. Currently, anthracene and its derivatives are much investigated[19–21] and frequently used in OLEDs[22] and in other organic thin-layer-based electronic devices such as transistors[21] and photovoltaic cells.[23] In contrast, although much attention has been paid to anthracene-based, fully conjugated polymers such as polyanthrylenes,[24] and poly(anthrylene vinylene)s,[25] relatively little work describing the exploitation of these materials in electronic devices has been reported. The main limitation has been the poor solubility of

*Correspondence to:* M. Majdoub (mustapha.majdoub@fsm.rnu.tn).

Contract grant sponsor: Ministry of Higher Education and Scientific Research of Tunisia; contract grant number: CMCU 05S1304.

such rigid polymers, which leads to processing difficulties in thin-layer preparation by the spin-coating technique. Another drawback of these systems is the high crystallinity of the anthracene units, which prevents the formation of stable, flexible films. To solve these problems, Cui et al.[26] incorporated flexible aliphatic side chains into the anthracene units. Soluble poly(9,10-bialkynyl anthrylene)s were thus synthesized, and a thin-film field-effect transistor was elaborated. Another successful route to soluble anthracene-based semiconducting polymers is the introduction of the anthracene unit into the macromolecular structure of a usually soluble conjugated polymer such as substituted poly(*p*-phenylene), poly(*p*-phenylene vinylene), or polythiophene. The investigation of the obtained copolymers showed improved thermal stability and a higher photoluminescence (PL) quantum yield in comparison with the corresponding usual polymers. Considerable interest has also been devoted to conjugated–nonconjugated block copolymers in which anthracene-based conjugated units are connected by solubilization of nonconjugated spacer segments. With various types of spacer groups, different soluble, anthracene-containing polyamides,[27] polyesters,[28] and polyurethanes[29] have been reported. A series of polymers containing anthracene units linked with flexible alkyl chains, including poly(methylene anthrylene)[30] and poly(trimethylene anthrylene),[31] were also synthesized and exhibited significantly high PL quantum yields. We followed the same strategy, which benefited from the flexibility of the ether spacer groups, and we report the synthesis and characterization of new soluble, anthracene-based semiconducting polyethers for organic thin-layer electronic applications.

## EXPERIMENTAL

### Materials and measurements

4,4′-Isopropylidenediphenol [bisphenol A (BPA); Acros, Illkirch, France; 97%], 4,4′-(hexafluoroisopropylidene)diphenol [fluorinated bisphenol A (BPAF); Acros, Illkirch, France; 97%], anthracene (Fluka; Taufkirchen, Germany; 97%), potassium carbonate (Acros; 99%), and paraformaldehyde (Acros; 96%) were used as received. The commercially available solvents were used without purification. $^{1}$H- and $^{13}$C-NMR spectral data were obtained with a Bruker AV 300 spectrometer (Wissembourg, France). Fourier transform infrared (FTIR) spectra were obtained with a PerkinElmer BX FTIR system spectrometer (United States, California) via the dispersion of samples in KBr disks, and ultraviolet–visible (UV–vis) absorption spectra were obtained with a Cary 2300 spectrophotometer (Varian, Les Ulis, France). For PL, samples were excited with a pulsed nitrogen laser line at 337 nm, and their spectra were recorded on a Jobin Yvon TRIAX 190 spectrometer (South San Francisco, United States of America) coupled to a nitrogen-cooled charged coupling device camera. For solid-state measurements, the films were deposited onto a quartz substrate from a chloroform solution. All measurements were performed at room temperature. Cyclic voltammetry (CV) was performed on an EG&G model 273 potentiostat/galvanostat (Princeton Applied Research, Midland, Canada) in a three-electrode cell with a polymer film that was drop-cast onto an indium tin oxide (ITO) working electrode. The measurements were carried out at a scanning rate of 50 mV/s against a reference saturated calomel electrode (SCE) with 0.1*M* tetrabutylammonium perchlorate [$(n\text{-Bu})_4NClO_4$] in acetonitrile as the supporting electrolyte. The electrochemical cell was externally calibrated by a ferrocene standard. The measurements were performed at 25°C, and the cell was deoxygenated with argon before each scan.

### Synthesis of 9,10-dichloromethylanthracene (AnCl)

A mixture of anthracene (1.83 g, 10 mmol), paraformaldehyde (1.56 g, 50 mmol of $CH_2O$), and 37% aqueous HCl (5 mL, 60 mmol) in acetic acid (30 mL) was heated at 50°C for 24 h. The resulting mixture was then cooled to room temperature, poured into distilled water, and extracted with chloroform. The organic layer was washed several times with distilled water and dried over anhydrous magnesium sulfate. The obtained solution was then concentrated, and AnCl was obtained as a yellow powder by precipitation in diethyl ether.

Yield: 86%. $^{1}$H-NMR (300 MHz, $CDCl_3$, δ): 8.38 (dd, $^{3}J$ = 6.9 Hz, $^{4}J$ = 3.0 Hz, 4H, Ar—H), 7.66 (dd, $^{3}J$ = 6.9 Hz, $^{4}J$ = 3.0 Hz, 4H, Ar—H), 5.61 (s, 4H, $CH_2Cl$). $^{13}$C-NMR (75.5 MHz, $CDCl_3$, δ): 129.8, 129.8, 126.7, 124.4, 38.8. FTIR ($cm^{-1}$): 3086 (w, aromatic C—H stretching), 1517 (s, C=C stretching), 796 (s, aromatic C—H out-of-plane bending), 625 (s, C—Cl stretching).

### Synthesis of the anthracene/bisphenol A (An–BPA) polymer

To an equimolar stirred mixture of AnCl (0.275 g, 1 mmol) and BPA (0.235 g, 1 mmol) in 15 mL of dimethylformamide was added 0.552 g of potassium carbonate (4 mmol). After 24 h of stirring at 60°C, the reaction mixture was cooled to room temperature, poured into distilled water, and extracted with chloroform. The organic layer was washed several times with distilled water and dried over anhydrous magnesium sulfate. The solution was then concentrated, and a brown powder was obtained by precipitation in methanol. It was filtered and dried *in vacuo* for 24 h.

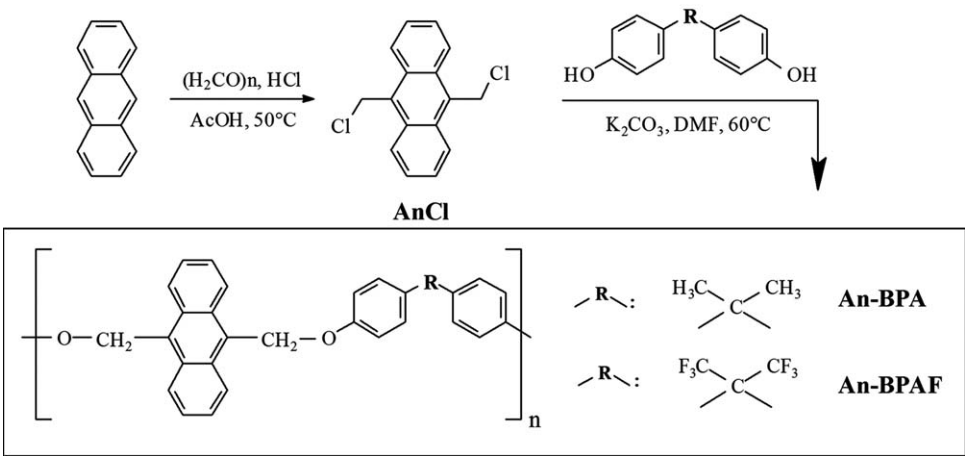


**Scheme 1** Synthetic route to polymers An–BPA and An–BPAF.

Yield: 55%. $^1$H-NMR (300 MHz, $CDCl_3$, δ): 8.37–6.78 (aromatic H), 5.96–5.94 ($OCH_2$), 4.30 (phenol end group), 1.77–1.70 ($CH_3$). $^{13}$C-NMR (75.5 MHz, $CDCl_3$, δ): 162.1–114.5 (aromatic C), 63.0 (PhOC), 42.3–42.2 [$C(CH_3)_2$], 31.7–31.5 ($CH_3$). FTIR ($cm^{-1}$): 3056, 3013, (w, aromatic C—H stretching), 2979, 2924, 2818 (w, aliphatic C—H stretching), 1519 (s, C=C stretching), 1250 (s, C—O—C asymmetric stretching), 1030 (m, C—O—C symmetric stretching), 750 (s, aromatic C—H out-of-plane bending).

### Synthesis of the anthracene/fluorinated bisphenol A (An–BPAF) polymer

To an equimolar stirred mixture of AnCl (0.275 g, 1 mmol) and BPAF (0.336 g, 1 mmol) in 15 mL of dimethylformamide was added 0.552 g of potassium carbonate (4 mmol). After 24 h of stirring at 60°C, the reaction mixture was cooled to room temperature, poured into distilled water, and extracted with chloroform. The organic layer was washed several times with distilled water and dried over anhydrous magnesium sulfate. The solution was then concentrated, and a yellow powder was obtained by precipitation in methanol. It was filtered and dried *in vacuo* for 24 h.

Yield: 53%. $^1$H-NMR (300 MHz, $CDCl_3$, δ): 8.37–6.87 (aromatic H), 6.02–5.96 ($OCH_2$), 4.30 (phenol end group, Ph—OH). $^{13}$C-NMR (75.5 MHz, $CDCl_3$, δ): 163.0–114.6 (CF and aromatic C), 63.2 (PhOC), 51.2 [C—$(CF_3)_2$]. FTIR ($cm^{-1}$): 3102, 3059, (w, aromatic C—H stretching), 2924, 2896 (w, aliphatic C—H stretching), 1519 (s, C=C stretching), 1250 (s, C—O—C asymmetric stretching), 1170 (s, C—F symmetric stretching), 1030 (m, C—O—C symmetric stretching), 750 (s, aromatic C—H out-of-plane bending).

### Fabrication and characterization of the diodes

Single-layer devices were fabricated as sandwich structures between an aluminum cathode and an ITO anode. A polymer solution ($2 \times 10^{-2} M$ in chloroform) was spin-cast (2000 rpm) onto ITO glass to obtain a film about 40 nm thick after 1 h of annealing at 40°C. A thin aluminum layer (150 nm) was deposited by thermal evaporation at $3 \times 10^{-6}$ Torr. The current–voltage characteristics of the devices were recorded with a Keithley 236 source meter (GIF SUR YVETTE, France). Devices were fabricated and characterized in air at room temperature.

## RESULTS AND DISCUSSION

### Synthesis and structural characterization

The anthracene-based polyethers were obtained by the two-step synthetic route shown in Scheme 1. AnCl was synthesized by direct chloromethylation of anthracene with the HCl/paraformaldehyde/acetic acid system according to a general procedure previously described for aromatic compound chloromethylation.[32,33] The polymers were synthesized via the Williamson reaction[34] through the polycondensation of AnCl with two different bisphenols; thus, the reaction of AnCl with BPA led to An–BPA, whereas An–BPAF was obtained from AnCl and BPAF. The polyethers were found to have good solubility in common organic solvents such as tetrahydrofuran, chloroform, and methylene chloride. The polymer structures were confirmed by NMR and FTIR spectroscopic analysis. $^1$H-NMR spectra (Fig. 1) showed a broad peak between 8.50 and 6.50 ppm that was assigned to aromatic protons. The $CH_2O$ groups appeared in the range of 6.00–5.95 ppm. The BPA methyl groups yielded a peak at 1.54 ppm. The absence of chloromethyl peaks (5.63 ppm) and the existence of a signal at approximately 4.30 ppm suggested total phenol end groups (Ph—OH). The FTIR spectra showed absorption bands due to aromatic and aliphatic C—H stretching between 3015 and 2815 $cm^{-1}$. The aromatic ring C=C stretching

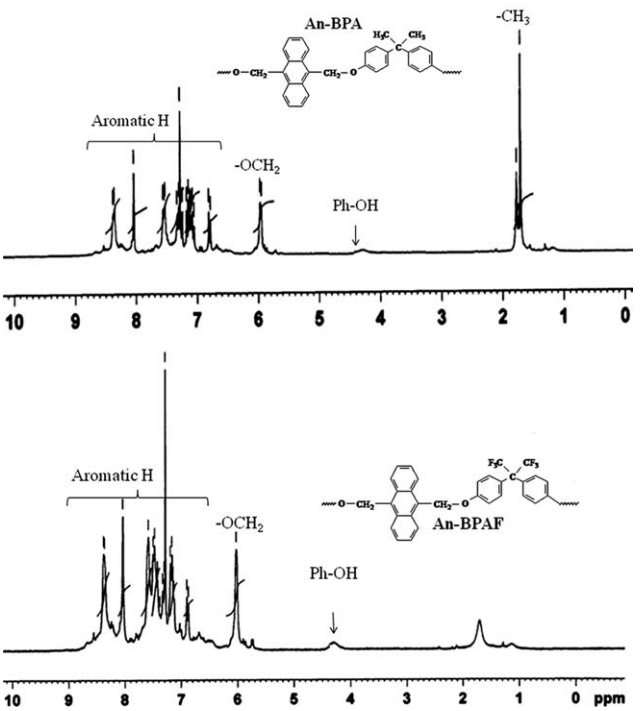


**Figure 1** $^1$H-NMR spectra of An–BPA and An–BPAF.

vibrations appeared at approximately 1500 $cm^{-1}$. The strong band at 1250 $cm^{-1}$ was attributed to the asymmetric C—O—Ar stretching vibration, and the band at approximately 1030 $cm^{-1}$ was assigned to the symmetric C—O—Ar vibration. The out-of-plane bending vibration of the aromatic hydrogens explained the strong absorption band at approximately 750 $cm^{-1}$. The An–BPAF spectrum included a strong band at 1170 $cm^{-1}$ that was attributed to the symmetric C—F vibration. The number-average molecular weights of the polymers were evaluated by a comparison of the $^1$H-NMR signal integrations for the phenol end groups and $OCH_2$ units. The weights were 2580 and 3240 for An–BPA and An–BPAF, respectively.

## Optical properties

The UV–vis absorption and PL spectra of the polyethers were recorded in diluted chloroform solutions and in thin solid films; Table I summarizes these spectral data.

In dilute solutions, the polymer absorption spectra showed similar features with three maxima at 356, 375, and 396 nm (Fig. 2). Evidently, these characteristic bands stemmed from the anthracene $\pi$–$\pi^*$ electronic transitions,[20] but even in dilute solutions, interactions between neighboring anthracene moieties of the same polyether chain can still be present and have to handled. Long ago, an important effort was devoted to determining the effects of intermolecular coupling

**TABLE I**
**Optical Data for An–BPA and An–BPAF**

| | Absorption | | PL | |
|---|---|---|---|---|
| | $\lambda_{max}$ (nm) | $\lambda_{onset}$ (nm) | $\lambda_{max}$ (nm) | fwhm (nm) |
| Dilute solution in chloroform | | | | |
| An–BPA | 356, 375, 396 | 429 | 390, 412, 438,[a] 467[a] | 71 |
| An–BPAF | 356, 375, 396 | 419 | 390, 412, 437, 467[a] | 40 |
| Thin film | | | | |
| An–BPA | 360, 380, 401 | 471 | 563 | 206 |
| An–BPAF | 360, 380, 401 | 430 | 504 | 204 |

$\lambda_{max}$ = wavelength of maximum absorption; $\lambda_{onset}$ = wavelength of absorption onset; fwhm = spectrum full width at half-maximum.
[a] Shoulder.

on aromatic molecular crystal spectra,[35] and it has been shown that the interactions depend mainly on the relative orientations and distances of molecules and on the values of electronic dipolar transition moments. For anthracene, the so-called 380-nm system is polarized along the molecular short axis and has moderate intensity (0.1 oscillator strength), so the order of magnitude of interactions at the relevant intrachain distances is rather moderate and probably shifts and broadens the transition bands by a few hundreds of inverse centimeters at the most. This evaluation agrees with our experimental spectra; however, the An-BAPF spectrum was narrower and more structured. Such behavior was probably due to the steric hindrance of the bulky fluoromethyl groups, which blocked the conformational changes and consequently reduced the available vibrational and rotational freedom degrees in An–BPAF.[36] This hindrance could increase to keep fixed the relative distances and orientations of anthracene in consecutive unit cells of the chain and favor a specific interaction value; this could be the cause of the shoulder around 420 nm observed

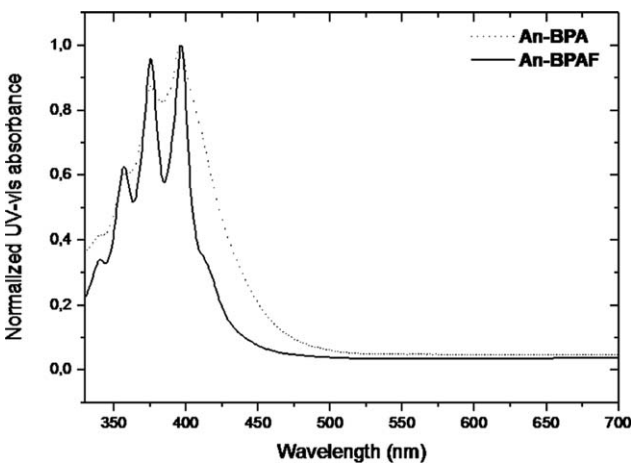


**Figure 2** UV–vis absorption spectra of An–BPA and An–BPAF [dilute solutions in chloroform ($5 \times 10^{-5} M$)].

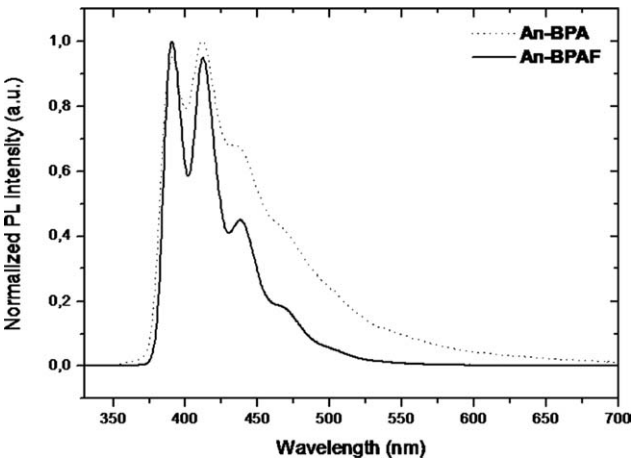


**Figure 3** PL spectra of An–BPA and An–BPAF [dilute solutions in chloroform ($2 \times 10^{-7}M$)].

for this compound. In contrast, the anthracene positions in An–BPA chains would be more randomized, with no emergence of precise conformations. Likewise, the steric effect influenced the solution emissions, and the polyethers presented practically the same blue PL spectra, with a narrower spectrum for the fluorinated polyether (Fig. 3). The absorption and emission spectra showed the mirrorlike aspect characteristic of rigid, condensed aromatic hydrocarbons.

In the solid state, the absorption spectra were only slightly redshifted by the proximity of anthracene moieties from other neighboring chains (Fig. 4). The new interchain interactions brought about additional broadening of An–BPA and An–BPAF bands. Similar behavior is in fact generally observed in π-conjugated polymers and has been attributed to the π–π stacking of conjugated segments and aggregate formation in the solid state.[37] In the case of the An–BPAF film, we noted a lower redshift of the absorption onset (11 nm). These results suggested weaker π–π interactions between anthracene in comparison with An–BPA. The

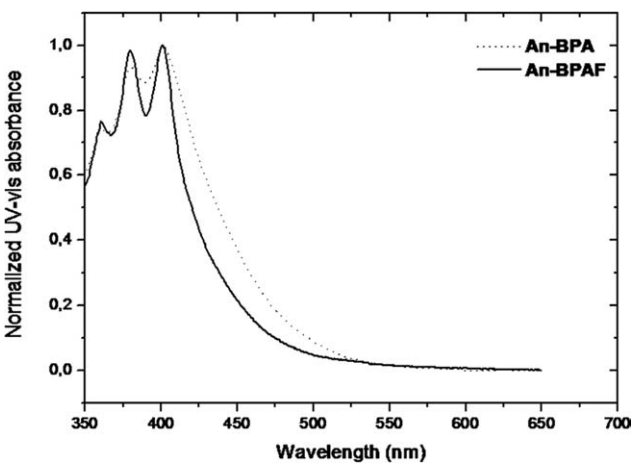


**Figure 4** UV–vis absorption spectra of An–BPA and An–BPAF in thin films (40 nm).

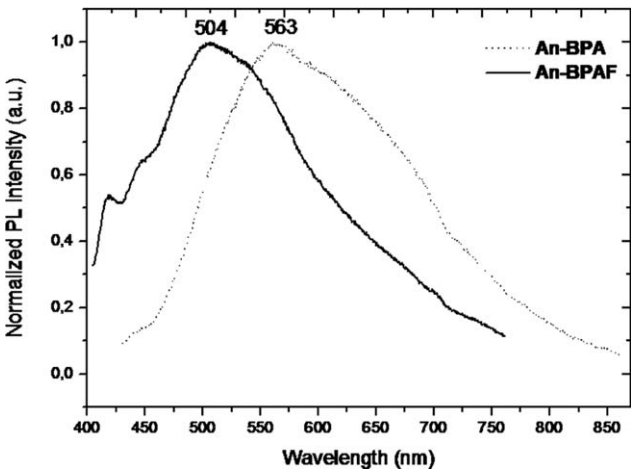


**Figure 5** PL spectra of An–BPA and An–BPAF in thin films (40 nm).

restriction of anthracene stacking was probably due to steric hindrance by the bulky hexafluoroisopropylidene groups.[38] The optical band gaps were estimated from the absorption onset of the polymer films. The calculated values were 2.63 and 2.88 eV for An–BPA and An–BPAF, respectively. The π–π stacking of conjugated moieties also influenced the film emission, and broad, redshifted PL spectra were obtained as a result to excimer formation[39] in comparison with the solution spectra (Fig. 5). An important redshift was observed for An–BPA, and a green-yellow emission was obtained (563 nm). In the case of the An–BPAF film, a smaller redshift was detected, and the green emission (504 nm) was more clearly a superimposition of isolated anthracene molecules and excimer emissions; this was again indicative of the larger intermolecular distances in An–BPAF.

In conclusion, electronic spectra in solution showed evidence of interactions between anthracene molecules belonging to the same chain; in the condensed phase, intrachain interactions further broadened the bands. The emission of films was dominated by excimer emission, and this testified to the close packing of anthracene, especially for the An–BPA compound less sterically hindered than An–BPAF.

### Highest occupied molecular orbital energy level ($E_{HOMO}$) and lowest unoccupied molecular orbital energy level ($E_{LUMO}$)

CV was employed to investigate the redox behavior of the polymers and to estimate their $E_{HOMO}$ and $E_{LUMO}$ values. In fact, knowledge of these energy levels is of crucial importance to the selection of cathode and anode materials for OLED devices.[40] The use of CV analysis is reliable because the electrochemical processes are similar to those involved in charge-injection and transport processes in OLEDs.[41] The polyether films were drop-coated onto an ITO glass

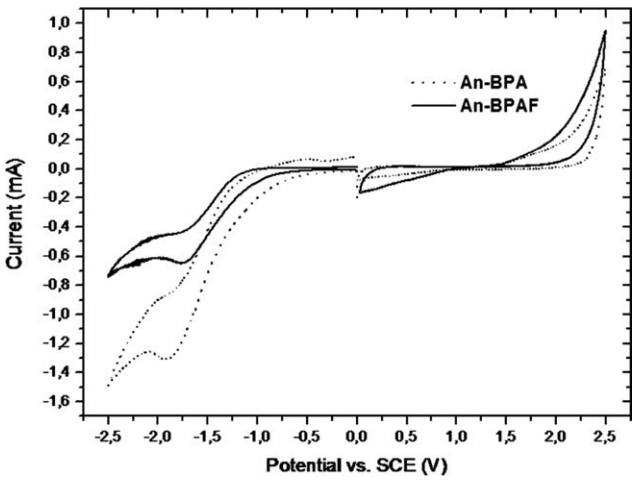


**Figure 6** Cyclic voltammograms for polyether films coated onto ITO electrodes in 0.1*M* $(n\text{-Bu})_4NClO_4$/acetonitrile (scan rate = 50 mV/s).

substrate and scanned both positively and negatively in $(n\text{-Bu})_4NClO_4$/acetonitrile. The obtained cyclic voltammograms are shown in Figure 6.

According to an empirical method,[42] under the assumption that the energy level of the ferrocene/ferrocenium couple was 4.8 V below the vacuum level, $E_{HOMO}$, $E_{LUMO}$, and the electrochemical gap [$E_{g\text{-}el}$ (eV)] were calculated as follows:

$$E_{HOMO}(\text{ionization potential}) = -(V_{\text{onset-ox}} - V_{FOC} + 4.8)$$

$$E_{LUMO}(\text{electron affinity}) = -(V_{\text{onset-red}} - V_{FOC} + 4.8)$$

$$E_{g\text{-}el} = E_{LUMO} - E_{HOMO}$$

**TABLE II**
**Electrochemical Data for An–BPA and An–BPAF**

| | $V_{\text{onset-ox}}$ (V) | $V_{\text{onset-red}}$ (V) | $E_{HOMO}$ (eV) | $E_{LUMO}$ (eV) | $E_{g\text{-}el}$ (eV) |
|---|---|---|---|---|---|
| An–BPA | 1.09 | −1.63 | −4.99 | −2.27 | 2.72 |
| An–BPAF | 1.97 | −1.08 | −5.87 | −2.82 | 3.05 |

where $V_{FOC}$ is the ferrocene half-wave potential (0.9 V), $V_{\text{onset-ox}}$ is the polymer oxidation onset, and $V_{\text{onset-red}}$ is the polymer reduction onset (all were measured versus SCE). The calculated $E_{HOMO}$, $E_{LUMO}$, and $E_{g\text{-}el}$ values are summarized in Table II. A higher $E_{g\text{-}el}$ value for the fluorinated polyether (An–BPAF) was estimated. A slight difference between the band gaps obtained by the optical method (the optical band gap) and by electrochemical analysis ($E_{g\text{-}el}$) was previously reported for some other conjugated polymers and was attributed to the interface barrier between the polymer film and the electrode surface.[39] In fact, the optical value corresponds to the pure band gap between the valence band and the conduction band, whereas the electrochemical value may be the result of the optical band gap coupled with the interface barrier for charge injection (this makes it larger).

## Electrical properties

Two single-layer devices with an ITO/polyether/aluminum configuration were fabricated to investigate the current–voltage characteristics of the anthracene-based polyethers. As shown in Figure 7, the current–voltage curves indicate typical diode behavior with relatively low turn-on voltages of 3.5 and

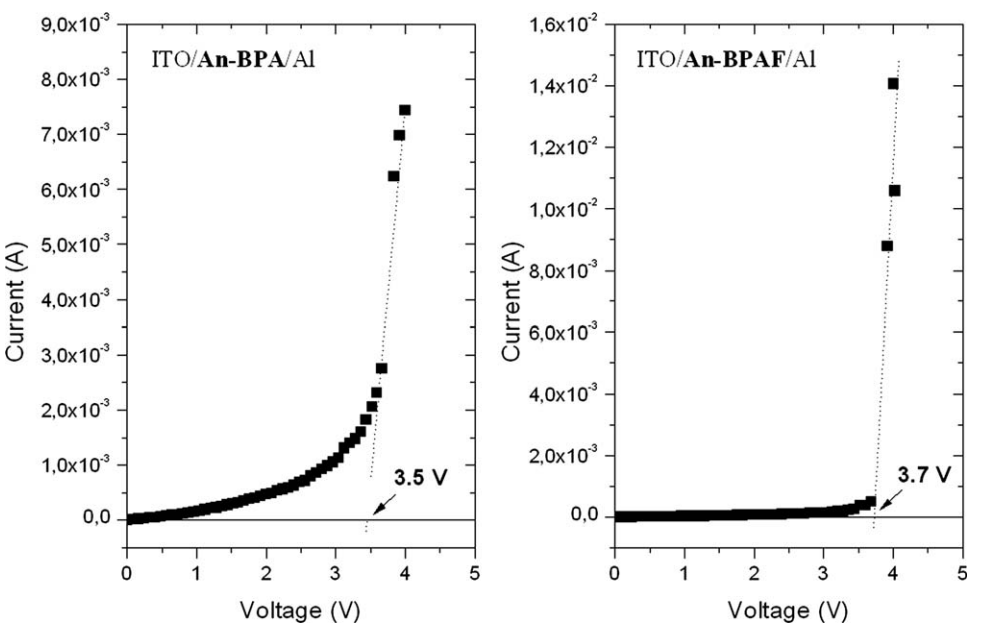


**Figure 7** Current–voltage curves for ITO/polyether/aluminum diodes.

3.7 V for An–BPA and An–BPAF, respectively. Nevertheless, no electroluminescence could be recorded for these simple devices. The reason was probably unbalanced charge injection, which increased the probability of radiationless exciton quenching at the electrode–polymer interface.[43] Therefore, we believe that the device turn-on voltage indicates the threshold of a hole-governed unipolar injection. Work is in progress to build electroluminescent multilayer devices.

## CONCLUSIONS

New soluble, anthracene-based polyethers (An–BPA and An–BPAF) were synthesized and characterized. In dilute solutions, the polymers presented similar blue emissions, with some evidence of intrachain interactions between anthracene moieties. In polymer films, the interchain π interactions influenced the optical behavior, and redshifted PL spectra were obtained: because of the presence of sizable amounts of anthracene excimer emission, a green emission was observed in An–BPAF, and a green-yellow emission was observed in An–BPA. The current–voltage characteristics of the devices with an ITO/polyether/aluminum configuration demonstrated typical diode behavior and relatively low turn-on voltages. All these features make these polymers promising active materials for anthracene-based OLEDs.

The authors thank Rafik Ben Chaâbane and Haikel Hrichi (Laboratoire de Physique et Chimie des Interfaces, Faculté des Sciences de Monastir) for the electrical measurements and Amna Debbebi (Faculté des Sciences de Monastir) for the NMR measurements. Special thanks go to John Lomas for his help in improving the quality of the English of this article and for his scientific remarks.

## References

1. Hung, L. S.; Chen, C. H. Mater Sci Eng Rep 2002, 39, 143.
2. Sun, Y.; Liu, Y.; Zhu, D. J Mater Chem 2005, 15, 53.
3. Lo, S. C.; Burn, P. L. Chem Rev 2007, 107, 1097.
4. Segura, J. L. Acta Polym 1998, 49, 319.
5. Akcelrud, L. Prog Polym Sci 2003, 28, 875.
6. Murphy, A. R.; Fréchet, J. M. J. Chem Rev 2007, 107, 1066.
7. Ando, S.; Nishida, J. I.; Fujiwara, E.; Tada, H.; Inoue, Y.; Tokito, S.; Yamashita, Y. Chem Mater 2005, 17, 1261.
8. Thompson, B. C.; Fréchet, J. M. J. Angew Chem Int Ed 2008, 47, 58.
9. Thomas, S. W.; Joly, G. D.; Swager, T. M. Chem Rev 2007, 107, 1339.
10. Lange, U.; Roznyatovskayal, N. V.; Mirsky, V. M Anal Chim Acta 2008, 614, 1.
11. Samuel, I. D. W.; Turnbull, G. A. T. Chem Rev 2007, 107, 1272.
12. Kraft, A.; Grimsdale, A. C.; Holmes, A. B. Angew Chem Int Ed Eng 1998, 37, 402.
13. Hughes, G.; Bryce, M. R. J Mater Chem 2005, 15, 94.
14. Walzer, K.; Maennig, B.; Pfeiffer, M.; Leo, K. Chem Rev 2007, 107, 1233.
15. Pope, M.; Kallman, H.; Magnante, P. J Chem Phys 1963, 38, 2042.
16. Dresner, J.; Goodman, A. M. (to RCA Corp.). U.S. Pat. 3,710,167 (1973).
17. Williams, D. F.; Schadt, M. J Chem Phys 1970, 53, 3480.
18. Vincett, P. S.; Barlow, W. A.; Hann, R. A.; Roberts, G. G. Thin Solid Films 1984, 94, 171.
19. Ben Chaâbane, R.; Jaballah, N.; Benzarti-Ghédira, M.; Chaieb, A.; Majdoub, M.; Ben Ouad, H. Phys B 2009, 404, 1912.
20. Gondek, E.; Kityk, I. V.; Danel, A. Mater Chem Phys 2008, 112, 301.
21. Meng, H.; Sun, F.; Goldfinger, M. B.; Gao, F.; Londono, D. J.; Marshal, W. J.; Blackman, G. S.; Dobbs, K. D.; Dalen, E. K. J Am Chem Soc 2006, 128, 9304.
22. Raghunath, P.; Ananth Reddy, M.; Gouri, C.; Bhanuprakash, K.; Jayathirtha, R. V. J Phys Chem A 2006, 110, 1152.
23. Valentini, L.; Bagnis, D.; Marrocchi, A.; Seri, M.; Taticchi, A.; Kenny, J. M. Chem Mater 2008, 20, 32.
24. Hodge, P.; Power, G. A.; Rabjohns, M. A. Chem Commun 1997, 73.
25. Garay, R. O.; Naarmann, H.; Müllen, K. Macromolecules 1994, 27, 1922.
26. Cui, W.; Zhang, X.; Jiang, X.; Tian, H.; Yan, D.; Geng, Y.; Jing, X.; Wang, F. Org Lett 2006, 8, 785.
27. Mikroyannidis, J. A. Polymer 2000, 41, 8193.
28. Jones, J. R.; Liotta, C. L.; Collard, D. M.; Schiraldi, D. A. Macromolecules 1999, 32, 5786.
29. Fomine, S.; Marin, M.; Fomina, L.; Salcedo, R.; Sansores, E.; Mendez, J. M.; Jimenez, C. F.; Ogawa, T. Polym J 1996, 28, 641.
30. Rameshbabu, K.; Kim, Y.; Kwon, T.; Yoo, J.; Kim, E. Tetrahedron Lett 2007, 48, 4755.
31. Bender, D.; Przybylski, M.; Müllen, K. Makromol Chem 1989, 190, 2071.
32. Jaballah, N.; Majdoub, M.; Fave, J. L.; Barthou, C.; Jouini, M.; Tanguy, J. Eur Polym J 2008, 44, 2886.
33. Trad, H.; Majdoub, M.; Davenas, J. Mater Sci Eng C 2006, 26, 334.
34. Jaballah, N.; Trad, H.; Majdoub, M.; Jouini, M.; Roussel, J.; Fave, J. L. J Appl Polym Sci 2006, 99, 2997.
35. Henari, F. Z.; Manaa, H.; Kretsch, K. P.; Blau, W. J.; Rost, H.; Pfeiffer, S.; Teuschel, A.; Tillmann, H.; Horhold, H. H. Chem Phys Lett 1999, 307, 163.
36. Craig, D. P.; Walmsley, S. H. Excitons in Molecular Crystals; Benjamin: New York, 1968.
37. Peng, K. Y.; Chen, S. A.; Fann, W. S.; Chen, S. H.; Su, A. C. J Phys Chem B 2005, 109, 9368.
38. Jaballah, N.; Hriz, K.; Majdoub, M.; Jouini, M.; Fave, J. L. High Perform Polym 2010, 22, 483.
39. Huang, Y. F.; Shiu, Y. J.; Hsu, J. H.; Lin, S. H.; Su, A. C.; Peng, K. Y.; Chen, S. A.; Fann, W. S. J Phys Chem C 2007, 111, 5533.
40. Fan, B.; Sun, Q.; Song, N.; Wang, H.; Fan, H.; Li, Y. Polym Adv Technol 2006, 17, 145.
41. Cheng, M.; Xiao, Y.; Yu, W. L.; Chen, Z. K.; Lai, Y. H.; Huang, W. Thin Solid Films 2000, 363, 110.
42. Bredas, J. L.; Silbey, R.; Bordeaux, D. S.; Chance, R. R. J Am Chem Soc 1983, 105, 6555.
43. Blom, P. W. M.; Vissenberg, M. C. J. M. Mater Sci Eng Rep 2000, 27, 53.